A Rapid-formed Supramolecular Polypeptide-DNA Hydrogel for *in-situ* Multi-layer 3D Bioprinting

Chuang Li[1], Alan Faulkner-Jones[2], Alison R. Dun[2], Juan Jin[1], Ping Chen[3], Yongzheng Xing[1], Zhongqiang Yang[1], Zhibo Li[3], Wenmiao Shu[2,*], Dongsheng Liu[1,*] and Rory R. Duncan[2]

Abstract: A rapid-formed supramolecular polypeptide-DNA hydrogel is prepared and applied for *in-situ* multi-layer 3D bioprinting for the first time. The hydrogel can be rapidly *in-situ* formed (in seconds) under physiological conditions by alternative deposition of two complementary bio-inks. Based on the dynamically crosslinked supramolecular hydrogel network, the printed structures via layer-by-layer assembly can merge and heal together, thus resulting in geometrically uniform and structurally precise constructs without obvious boundaries or defects. Owing to the high mechanical strength and non-shrinking/non-swelling properties of the hydrogel, the printed structures can keep their shapes in milimeter-scale without collapse or deformation. Furthermore, cell printing is demonstrated for fabrication of living-cell-containing structures with high viability and normal cellular functions. Together with the unique properties of biocompatibility, permeability and biodegradability, the hydrogel is an ideal soft material for 3D inkjet bioprinting to produce desired complex 3D constructs for tissue engineering application.

Bioprinting has attracted wide-spread attentions in tissue engineering as a powerful fabrication method to design and create tissue-like artificial structures and constructs.[1] Selecting a suitable scaffold material is one of the critical requirements for bioprinting.[1b, 2] Hydrogel has been widely explored among many scaffold materials due to its similarity to natural extra-cellular matrix (ECM) thus providing structural and physical supports for the encapsulated cells similar to natural environment.[3] So far, non-covalently crosslinked hydrogels from natural products including alginate, chitosan, collagen, matrigel, gelatin and agarose have been used in vitro as scaffold materials for bioprinting,[4] however, drawbacks such as thermal-triggered hydrogel formation, shrinking-induced shape deformation, limitation of responsiveness and tailorability hinder their further application in 3D bioprinting with living cells. Alternatively, covalently crosslinked hydrogels from synthetic products including poly(ethylene glycol) (PEG), polypeptides, poly(N-isopropylacrylamide) and pluronics emerged as appealing candidates because of their well-defined structures with possibilities to fine-tune their responsive properties.[5] However, shortages such as harsh reaction condition, lacking of specific biodegradability and biocompatibility, inability of self-healing between layers limit their applications in *in-situ* multi-layer 3D bioprinting with living cells. Therefore, development of novel bioprinting scaffold materials fulfilling the above requirements is consistently needed but also challenging. DNA is an excellent building scaffold to construct versatile devices and materials,[6] especially DNA hydrogels, which possess advantages such as designable responsiveness (pH, temperature, enzyme, aptamer and light et. al.),[7] non-swelling and non-shrinking property, biodegradability and permeability of nutrients.[7f] Previous reported applications such as cell-free protein production,[8] covers for single cell capture and release,[7f] ions detection,[7d, 9] etc, were only based on part of the these unique properties of DNA hydrogels. However, application based on all these unique properties fulfilling the requirements for 3D bioprinting has not been explored yet.

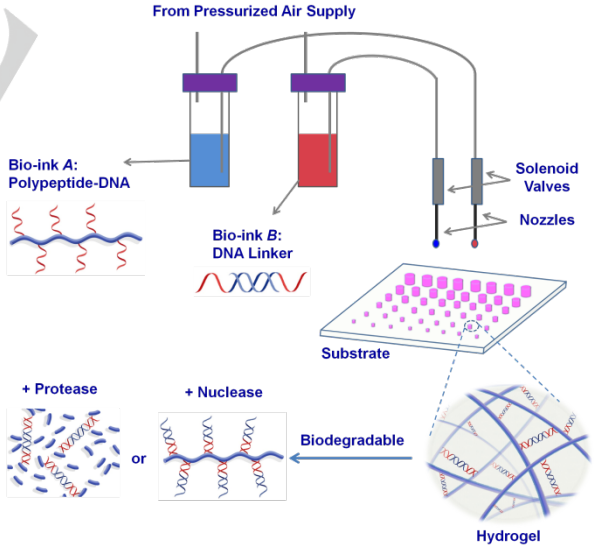

Scheme 1. 3D bioprinting process of polypeptide-DNA hydrogel to fabricate arbitrary designed 3D structures. There are two bio-inks, "bio-ink ***A***" (blue) is polypeptide-DNA; "bio-ink ***B***" (red) is DNA linker. The DNA sequences of bio-ink ***A*** and bio-ink ***B*** are complementary, and hybridization will cause crosslinking, leading to the hydrogel formation (pink). The formed hydrogels are responsive to both protease and nuclease, resulting in full degradation of the hydrogel networks on-demand after printing.

In this manuscript, we show for the first time a rapid *in-situ* multi-layer 3D bioprinting with DNA-based hydrogels as bioinks.

[a] [1] C. Li, Dr. J. Jin, Dr. Y. Xing, Prof. Z. Yang, Prof. D. Liu*
Key Laboratory of Organic Optoelectronics & Molecular Engineering of the Ministry of Education
Department of Chemistry
Tsinghua University, Beijing 100084, China
E-mail: liudongsheng@tsinghua.edu.cn

[b] [2] A. Faulkner-Jones, Dr. A. R. Dun, Dr. W. Shu*, Prof. R. R. Duncan
Institute of Biological Chemistry, Biophysics and Bioengineering
Heriot-Watt University, Edinburgh EH14 4AS, UK
Email: w.shu@hw.ac.uk

[c] [3] Dr. P. Chen, Prof. Z. Li
Beijing National Laboratory for Molecular Sciences (BNLMS)
Institute of Chemistry, Chinese Academy of Sciences
Beijing 100190, China

Supporting information for this article is given via a link at the end of the document.((Please delete this text if not appropriate))

As shown in **Scheme 1**, the DNA hydrogel contains two components: polypeptide-DNA conjugate (named bio-ink ***A***) and complementary DNA linker (named bio-ink ***B***). The mixture of bio-ink ***A*** and bio-ink ***B*** with a desired molar ratio leads to the rapid *in-situ* hydrogel formation (in seconds) under physiological conditions. By alternate deposition of bio-ink ***A*** and bio-ink ***B*** in the programmed position, designed 3D structures containing viable and functional living cells could be constructed. The resultant hydrogel exhibits these combined favourable properties from both polypeptide- and DNA-components, i.e. responsiveness to protease and nuclease, leading to the full biodegradation and removal of the hydrogel networks under physiological conditions after printing.

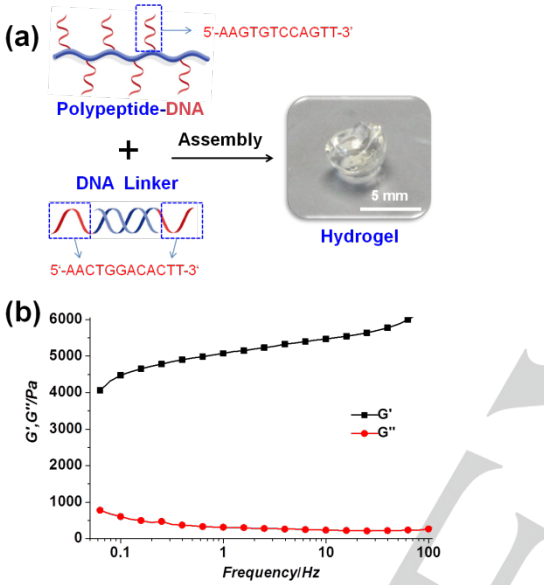

Figure 1. (a) Preparation of polypeptide-DNA hydrogel via a two-component-mixing of "bio-ink ***A***" and "bio-ink ***B***". **(b)** Rheological characterization of a hydrogel (5 wt%) and the frequency sweep test was carried out between 0.05 and 100 Hz at a fixed strain of 1 % at 25 °C.

As illustrated in **Figure 1a**, the hydrogel can be fabricated by a two-component mixing strategy: bio-ink ***A*** is a polypeptide-DNA conjugate, which was synthesized by grafting multiple single stranded DNAs (ssDNAs) onto polypeptide backbone via Cu^{+} catalyzed "click chemistry" between azide-DNA and poly(L-glutamic acid$_{240}$-co-γ-propargyl-L-glutamate$_{20}$) (p(LGA$_{240}$-co-PLG$_{20}$), M_w 34060, PDI 1.4) following an established method (detailed procedure see Supporting Information, Scheme S1).[7i] On average, 5-6 ssDNAs were conjugated to each polypeptide backbone (see Supporting Information, Figure S1), resulting in sufficient crosslinking points. Alternatively, bio-ink ***B*** is a double stranded DNA (dsDNA) containing two "sticky ends" with exactly the same sequences (see Supporting Information, Figure S2) which are complementary to that of ssDNA grafted onto polypeptides in bio-ink ***A*** (detailed sequences see Table S1). To check whether the hydrogel could be formed as designed, two bio-inks were mixed together at a 1:1 molar ratio of "sticky ends" with a final total mass content of 5 wt% in 1 × TBE buffer (pH 8.3, NaCl of 200 mM). It was found that due to the hybridization of the complementary DNA sequences, the mixture changed rapidly from a fluidic solution into an optically transparent supramolecularly crosslinked network within seconds, namely a polypeptide-DNA hydrogel (**Figure 1a**). It is worthy to mention that the hydrogel can be formed under physiological conditions (e.g. NaCl of 150 mM, pH 7.4, Figure S3), which is desirable for applications where the hydrogels have to be formed *in situ* with living cells. The formation of the hydrogel was further verified by oscillatory shear rheological tests. As shown in **Figure 1b**, the frequency sweep test was carried out between 0.05 Hz and 100 Hz at a fixed strain of 1 % at 25 °C and G' was significantly higher than G'' in the entire frequency range, indicating the hydrogel was indeed formed as designed. It is notable that the G' was high (~5000 Pa), resulting in a self-supported and free standing hydrogel with millimeter scale (Figure 1a).

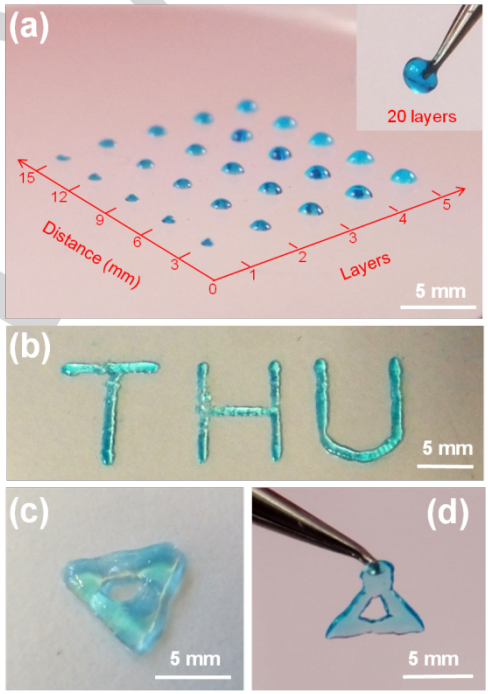

Figure 2. 3D printing of polypeptide-DNA hydrogel into 3D structures with blue dye added for visualization: **(a)** an array of printed droplets with an increasing gradient of layers. Inset, a lifted hydorgel with 20 layers; **(b)** the letters "THU" printed with 5 layers; **(c-d)** a triangle printed with 10 layers, **(d)** shows that the printed hydrogel structure is strong enough to be picked up with tweezers.

The unique two-component mixing strategy and rapid hydrogel forming property can fulfill the requirements for 3D ink-jet bioprinting which is a promising free-form fabrication method to produce tissue-like soft scaffolds and structures with living cells.[4e] As shown in **Figure 2**, equal amounts of bio-ink ***A*** (polypeptide-DNA conjugate, 6 wt%, 100 µl) and bio-ink ***B*** (DNA linker, 2 mM, 100 µl) were loaded into two separate printing cartridges of a microvalve-based 3D bioprinter, which we demonstrated recently to be able to print in 3D even the most difficult-to-culture cells such as stem cells, whilst maintaining cell viability and function.[10] By alternating printing nano- or micro-

droplets of bio-ink ***A*** and bio-ink ***B*** from the nozzles on the same spot, contact and hence mergence lead to the rapid *in situ* hydrogel formation based on the hybridization of complementary DNA sequences. Through designing of programmes, different 3D tissue-like patterns and structures with desired scales and dimensions could be constructed via the ink-jet bioprinter based on this "bottom-up" assembly strategy. **Figure 2a** shows a printed array of hydrogel droplets with an increasing gradient of sizes with blue dye added for visualization. The smallest size of the printed hydrogel droplet was estimated to be around 500 μm in diameter, 80 μm in thickness, 60 nl in volume. Note that the 3D printed hydrogel formation was very rapid (within seconds), which is probably facilitated by the small volume of the printed droplets and hence smaller diffusion distance. Interestingly, not only the volume and scale of one hydrogel droplet are precisely controllable, but also the location and distance between different hydrogel droplets are geometrically tunable by design of corresponding programs. Due to crosslinking by rigid DNA duplex, the printed hydrogel droplets show no obvious shrinking or swelling phenomenon, avoiding the possibility of shape deformation after printing. Furthermore, hydrogel droplets with 20 layers of printed inks were found to be mechanically strong enough to be manipulated physically (Figure 2a, inset). Apart from the droplet arrays, designable hydrogel structures such as alphabetic letters "THU" (**Figure 2b**) and a simple triangle (**Figure 2c**) were 3D printed following the above "bottom-up" printing process, demonstrating the ability of our system to print arbitrary 3D structures. The hydrogel triangle structure (**Figure 2d**) could be manipulated without collapse, indicating that the mechanical strength of the 3D printed hydrogel is strong enough to support its printed shapes. Additionally, the printed structures are optically transparent and geometrically uniform without obvious boundaries and defects between the printed layers. This is due to the fact that the contacting layers of the hydrogel can further merge and heal together based on the supramolecularly dynamic crosslinking of DNA hybridization. It is concluded that i) the two-bio-ink mixing deposition and rapid *in-situ* formation under physiological conditions makes the hydrogel an excellent material for 3D ink-jet printing; ii) based on the supramolecularly dynamic crosslinked hydrogel network, the printed structures by layer-by-layer assembly can merge and heal together, resulting in geometrically uniform constructs without obvious boundaries and defects; iii) owing to the strong mechanical strength, non-shrinking and non-swelling properties, the hydrogel keeps the printed shapes and structures without deformation. All these properties prove the hydrogel to be promising printing materials for fabrication of complex 3D constructs with precise and regular inner structures.

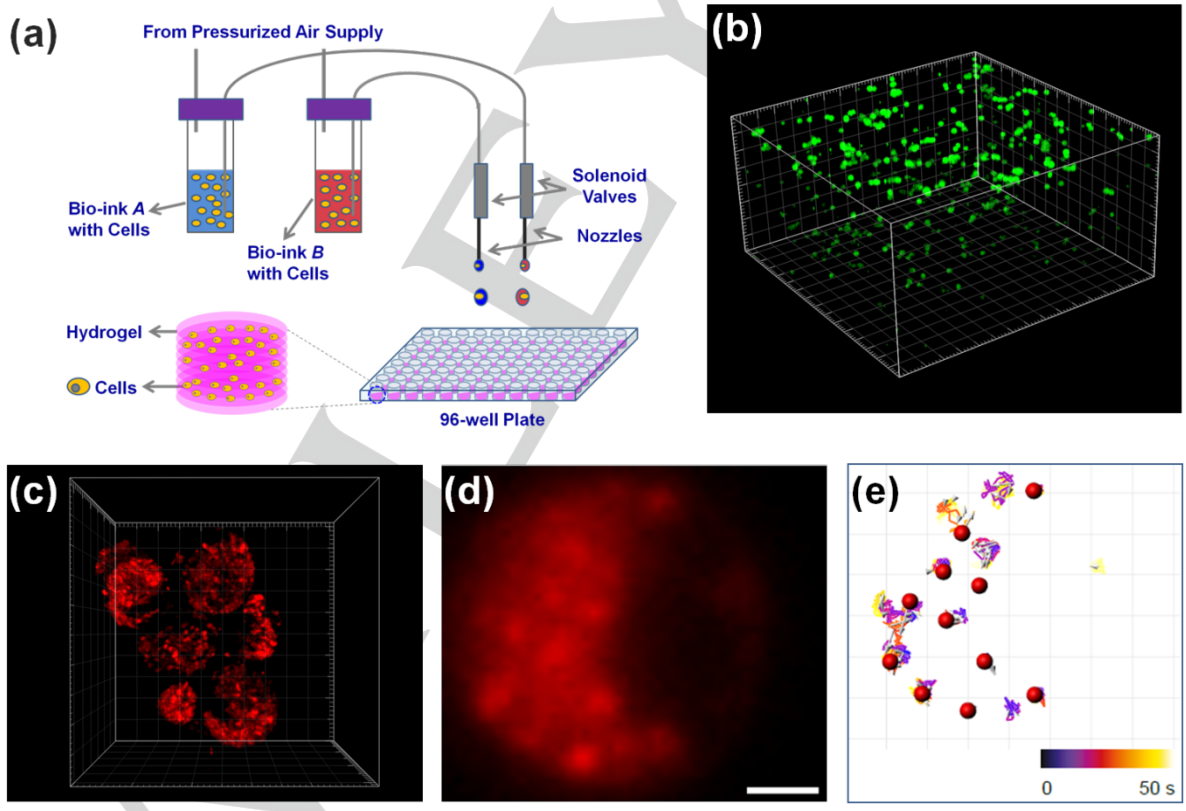

Figure 3. 3D bioprintings of polypeptide-DNA hydrogels with AtT-20 cells. **(a)** Schematic representation of cell printing process based on ink-jet technique. **(b)** A 3D stack of AtT-20 cells printed in hydrogel with FDA staining in green. Gridlines are 50 μm. **(c)** A 3D stack (at higher magnification) of AtT-20 cells printed in hydrogel and stained with Lysotracker-Red. Gridlines are 5 μm. **(d)** AtT-20 cells printed in hydrogel and stained with Lysotracker-Red were imaged using widefield microscopy, a cross section of the cells shows acidic compartments. Scale bar 1 μm. **(e)** Dynamic organelles were tracked and trajectories from inside the cell in **(d)** are shown. The tracked organelles are shown as red spheres and tracks as coloured lines with displacement indicated by grey arrows. Colour bar and colour of tracks represents time in seconds (0 - 50 seconds). Gridlines are 1 μm.

Next we applied the hydrogels in cell printing which offers the possibility to build 3D structures of cells for studying cell interactions and building artificial organs.[1a] Here AtT-20 cell (an anterior pituitary cell-line) was chosen as a model cell line for the cell printing study as it was widely used to investigate the intracellular transport, packaging, and secretion of hormones. As shown in **Figure 3a**, when AtT-20 cells were added into two bio-inks with a proper cell density, it was found that the bio-inks maintained a stable and homogenous cell suspension, preventing the settlement and aggregation of cells that usually impedes cell printing. This maybe benefit from the suitable viscosity and surface tension of the bio-inks which not only maintain cell suspension state but also meet the stringent fluid property needed for printing from the nozzle. We further carried out a thorough characterisation of the viability and function of AtT-20 cells after printing within the hydrogel in 3D. **Figure 3b** shows printed AtT-20 cells in the hydrogel stained with FDA and imaged using a laser-scanning confocal microscope (CLSM); the live/dead assay reported printed cell viability of 98.8 ± 1.4 % (Mean ± SD), indicating the printing process have little damage to cells. In order to test the biological function of printed cells, we also observed single cells in 3D in the hydrogel stained with Lysotracker-Red at high resolution, revealing intracellular acidic compartments (in red; **Figure 3c**). These intracellular acidic compartments (including lysosomes and large dense-cored vesicles) were visualized within the cytosol of a printed AtT20 cell using an inverted widefield microscope (**Figure 3d**) and were tracked over time (**Figure 3e**). Organelle dynamics were measured indicating that the printed AtT-20 cells were viable, had normal morphology in 3D and performed cellular functions including proton pump activity, metabolic turnover and membrane trafficking.[11]

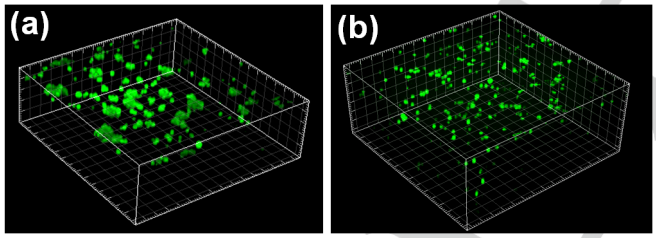

Figure 4. A 3-D stack of **(a)** AtT-20 cells and **(b)** HEK-293 cells in polypeptide-DNA hydrogel with FDA staining and imaged after 48 h. Gridlines are 50 µm.

To investigate the biocompatibility of the hydrogel with different cell types over different culture periods we employed polypeptide-DNA hydrogel as scaffolds for 3D cell culture (detailed procedure see Experimental Section). As shown in **Figure 4**, cultured cells were encapsulated and distributed in the hydrogels in 3D and the live-dead assays indicated the viability was 99.1 ± 1.7 % for AtT-20 cells (Figure 4a) and 99.3 ± 1.4 % for HEK-293 cells (Figure 4b) after 48 h culture. It was found that the viability of cells remained high at 95.8 ± 5.9 % even after 96 h of 3D culture in the hydrogel for HEK-293 cells, demonstrating that i) the hydrogel is mechanically strong enough to give physically environmental support for encapsulated cells distribution in 3D; ii) the hydrogel is non-toxic to cells and permeable for nutrients which are desirable for long-term cell culture.

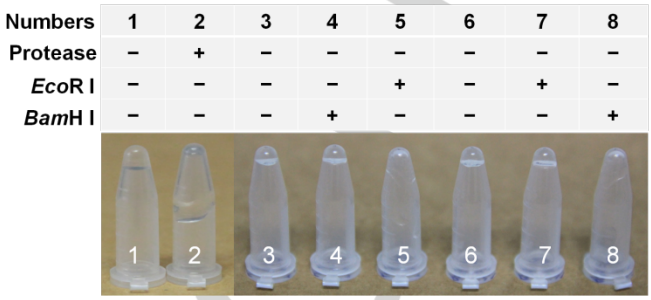

Figure 5. Enzymatic degradable behaviours of polypeptide-DNA hydrogels. **(1-2)** Protease responsiveness. 10 µl of 5 wt% hydrogel was incubated in 10 µl of phosphate buffer (pH 7.8) **(1)** without protease, **(2)** with 30 U Endoproteinase Glu-C at room temperature for 12 h. **(3-8)** Nuclease responsiveness. Hydrogel "R" **(3-5)** and hydrogel "H" **(6-8)** contain restriction sequences of *Eco*R I and *Bam*H I on their linkers, respectively. In each tube, 10 µl of 5 wt% hydrogel was incubated in 10 µl of reaction buffer **(3, 6)** without enzymes, **(4, 8)** with 30 U *Bam*H I, and **(5, 7)** with 30 U *Eco*R I at room temperature for 24 h.

In addition, we also studied the biodegradability of our hydrogel material which is critical and desirable for bioprinting. As shown in **Figure 5**, the hydrogel (5 wt%) can be degraded by endoproteinase Glu-C after incubation at room temperature for 12 h (tube 2). Alternatively, corresponding nuclease can cut DNA linker and digest the hydrogel network specifically. For example, after incabation at room temperature for 24h, hydrogels containing *Eco*R I restriction site (5'-GAATTC-3') remained in the gel-state in the absence of *Eco*R I restriction enzyme (tube 3 and tube 4), but turned into a solution when digested by the *Eco*R I restriction enzyme (tube 5). And *vice versa*, hydrogels containing *Bam*H I restriction site (5'-GGATCC-3') remained in the gel-state in the absence of *Bam*H I (tube 6 and tube 7), but dissolved when digested by *Bam*H I restriction enzyme (tube 8). These results indicated that the hydrogels possess highly specific dual-enzymatic responsiveness both to protease and nuclease, which can fully biodegrade both hydrogel backbone and crosslinker. Additionally, this offers the possibility of novel applications in tissue engineering where parts of the hydrogel should be selectively removed in the presence of cells to render specific 3D tissue structures.[12]

In summary, here we demonstrate a rapid-formed supramolecular polypeptide-DNA hydrogel and for the first time apply it to *in-situ* multi-layer 3D bioprinting. The two-bio-ink mixing deposition and rapid *in-situ* forming (in seconds) under physiological conditions make the hydrogel an ideal material for 3D ink-jet printing. Based on the dynamic crosslinking of DNA hybridization, the printed hydrogels possess excellent merging and healing properties, resulting in geometrically uniform constructs without boundaries. Furthermore, the printed structures can keep their shapes in milimeter-scale without collapse or deformation benefiting from the high mechanical strength and non-swelling/shrinking properties of the hydrogel. Cellular biocompatibility and permeability of nutrients make it

possible for cell printing to produce living-cell-containing structures with high viability and normal cellular functions. Designable biodegradability by dual-enzymatic responsiveness to protease and nuclease provides the possibility of complete removal of hydrogel networks on-demand from systems. All these properties above make the hydrogel a promising printing material for fabrication of desired complex 3D tissue-like constructs in tissue engineering.

Experimental Section

Synthesis of Bio-ink *A* (Polypeptide-DNA Conjugate). Polypeptide-DNA conjugate was synthesized via Cu^+ catalysed click chemistry following an established method.[7i]

Preparation of Bio-ink *B* (DNA Linker). Stoichiometric amounts of DNA strands were mixed in 1 × TBE buffer to give a final concentration of 5.0 mM for each DNA strand. The mixture was heated to 95 °C for 3 min and then cooled to room temperature over 2 h to form DNA linker.

Preparation of Polypeptide-DNA Hydrogels. A stock solution of two components was prepared: polypeptide-DNA conjugate (15 wt%, 13.8 mM with respect to grafted ssDNA) and DNA linkers (5 mM). Calculated volumes of the polypeptide-DNA conjugate and DNA linker solutions were added in 1.5 ml EP tubes in 1 × TBE buffer containing 200 mM NaCl and mixed quickly.

Rheological Tests. Rheological tests were carried out on an AR-G2 rheometer (TA Instruments). Two types of rheological experiments were performed in 8 mm parallel-plate geometry using 40 µl of hydrogels (resulting in a gap size of 0.15 mm): i) In order to find the linear viscoelastic region, oscillatory strain sweep (0.05 %-100 %) and frequency sweep (0.05 Hz-100 Hz) were conducted at 25 °C. The linear viscoelastic region was found to be in the range of 1 % strain and 1 Hz frequency; ii) Frequency sweep tests were carried out between 0.05 and 100 Hz at 25 °C at a fixed strain of 1 %.

3D Bioprinting. 100 µl each of bio-ink ***A*** (polypeptide-DNA conjugate, 6 wt%) and bio-ink ***B*** (DNA linker, 2 mM) were loaded into separate cartridges of Heriot-Watt University's valve-based bioprinter. Several test programs were created describing arrays and patterns in three-dimensions. These arrays and patterns were printed out on the printer by alternately printing of the bio-ink ***A*** and bio-ink ***B*** at the desired positions.

3D Cell Printing and Cell Function Test. AtT-20 cells (1×10^7 cells ml^{-1}, 20 µl) were added to bio-ink ***A*** (polypeptide-DNA conjugate, 6 wt%, 100 µl) which was loaded into the printer along with bio-ink ***B*** (DNA linker, 2 mM, 120 µl) in separate cartridges. 60 layers each of alternating bio-ink ***A*** with cells and bio-ink ***B*** with cells were printed in 4 samples. Two samples were stained with 40 µg/ml fluorescein diacetate (FDA) and 10 µg/ml propidium iodide (PI) in serum-free Dulbecco's Modified Eagle's Medium (DMEM) and incubated at 37 ºC in 5 % (v/v) CO_2, 95 % (v/v) air for 30 min. Images were acquired using a Leica SP5 SMD gated-STED confocal laser scanning microscope with either a 20X 0.7 NA HC PL APO objective or a 63X 1.3 NA HPX PL APO objective. Illumination was provided by an argon gas laser at 488 nm or a 561 nm diode laser and the sample was maintained at 37 °C in 5 % (v/v) CO_2 95 % (v/v) air for live cells. A fluorescent live/dead staining assay was used to calculate the viability of the cells. The remaining samples were stained with 100 nM Lysotracker-Red (Life Technologies) in serum-free DMEM and incubated at 37 ºC in 5 % (v/v) CO_2, 95 % (v/v) air for 30 min. prior to imaging with an inverted IX81 microscope (Olympus) using a 60X 1.45 NA UAPON TIRF objective with 561 nm excitation. 3D stacks were acquired with a z-step size of 2 µm (20X Lens) or 0.15 µm (63X Lens) and time-lapse recordings were acquired at 20 Hz.

3D Cell Culture. Both AtT-20 cells (5×10^6 cells ml^{-1}, 5 µl) and human embryonic kidney (HEK) 293 cells (5×10^6 cells ml^{-1}, 5 µl) were maintained on glass coverslips in polypeptide-DNA hydrogel (30 µl) at 37 ºC in 5 % (v/v) CO_2, 95 % (v/v) air in DMEM media containing 10 % (v/v) of foetal bovine serum, 0.1 % (v/v) Glutamax and 1 % (v/v) pen-strep. After cultured for the specified time, the cells were stained with 40 µg/ml FDA and 10 µg/ml PI and imaged using a Leica SP5 SMD gated-STED confocal laser scanning microscope. Image data were deconvolved using Huygens Professional (SVI, Netherlands) software and presented using Imaris (Bitplane, Northern Ireland). Viability was calculated by automatically identifying cells using the Imaris Spot Detection function and determining the relative proportion of live (green stained) or dead (red, PI stained) cells in each sample. At least 4 areas of view were measured and data are presented as mean values ± Standard Deviation.

Preparation of Nuclease Responsive Hydrogels. A stated bio-ink ***R*** (containing an *Eco*R I restriction site) and bio-ink ***H*** (containing a *Bam*H I restriction site) were separately mixed with a stated polypeptide-DNA conjugate to form hydrogel 'R' and hydrogel 'H' in corresponding reaction buffer: for *Eco*R I, the buffer contained 50 mM of Tris-HCl (pH 7.5), 100 mM of NaCl, 10 mM of $MgCl_2$ and 1 mM of dithiothreitol, whereas for *Bam*H I, the buffer contained 20 mM of Tris-HCl (pH 8.5), 100 mM of KCl, 10 mM of $MgCl_2$ and 1 mM of dithiothreitol.

Protease Cleavage of Hydrogels. 10 µl of polypeptide-DNA hydrogel was incubated with 30 U Endoproteinase Glu-C in 10 µl of the phosphate buffer at room temperature for 12 h.

Nuclease Cleavage of Hydrogels. 10 µl of polypeptide-DNA hydrogel was incubated with 30 U of *Eco*R I or 30 U of *Bam*H I in 10 µl of the corresponding reaction buffer at room temperature for 24 h.

Acknowledgements

We thank the National Basic Research Program of China (973 program, 2013CB932803), the National Natural Science Foundation of China (91427302, 21421064), the NSFC–DFG joint project TRR61, and the Beijing Municipal Science & Technology Commission for financial support. This project was also partly supported by the Sino–UK Higher Education Research Partnership for PhD Studies Scheme funded by the British Council and the Ministry of Education in China and EPSRC (EP/M506837/1) and MRC awards to R.R.D. (MRC_G0901607) and by the Wellcome Trust (WT074146). The MRC (MRC_MR/K01563X/1) Edinburgh Super-Resolution Imaging Consortium (ESRIC) provided the microscope platforms, technical assistance, tissue culturing facilities, and analysis packages required for the acquisition and analysis of fluorescence imaging data summarized in this article.

Keywords: DNA hydrogel • polypeptide • supramolecular • bioprinting • biodegradability

[1] a) P. Calvert, *Science* **2007**, *318*, 208-209; b) S. V. Murphy, A. Atala, *Nat. Biotech.* **2014**, *32*, 773-785; c) M. D. Symes, P. J. Kitson, J. Yan,

C. J. Richmond, G. J. T. Cooper, R. W. Bowman, T. Vilbrandt, L. Cronin, *Nat. Chem.* **2012**, *4*, 349-354; d) F. Pati, J. Jang, D.-H. Ha, S. Won Kim, J.-W. Rhie, J.-H. Shim, D.-H. Kim, D.-W. Cho, *Nat. Commun.* **2014**, *5*; e) N. G. Durmus, S. Tasoglu, U. Demirci, *Nat. Mater.* **2013**, *12*, 478-479.

[2] a) S. V. Murphy, A. Skardal, A. Atala, *J. Biomed. Mater. Res. A.* **2013**, *101A*, 272-284; b) M. Nakamura, S. Iwanaga, C. Henmi, K. Arai, Y. Nishiyama, *Biofabrication* **2010**, *2*, 014110.

[3] a) D. Seliktar, *Science* **2012**, *336*, 1124-1128; b) M. P. Lutolf, P. M. Gilbert, H. M. Blau, *Nature* **2009**, *462*, 433-441; c) J. L. Drury, D. J. Mooney, *Biomaterials* **2003**, *24*, 4337-4351; d) B. V. Slaughter, S. S. Khurshid, O. Z. Fisher, A. Khademhosseini, N. A. Peppas, *Adv. Mater.* **2009**, *21*, 3307-3329; e) E. A. Appel, J. del Barrio, X. J. Loh, O. A. Scherman, *Chem. Soc. Rev.* **2012**, *41*, 6195-6214; f) G. A. Silva, C. Czeisler, K. L. Niece, E. Beniash, D. A. Harrington, J. A. Kessler, S. I. Stupp, *Science* **2004**, *303*, 1352-1355; g) Y. Zhang, L. Tao, S. Li, Y. Wei, *Biomacromolecules* **2011**, *12*, 2894-2901.

[4] a) S. Khalil, W. Sun, *J. Biomech. Eng.* **2009**, *131*, 111002; b) J. C. Reichert, A. Heymer, A. Berner, J. Eulert, U. Nöth, *Biomed. Mater.* **2009**, *4*, 065001; c) K. Pataky, T. Braschler, A. Negro, P. Renaud, M. P. Lutolf, J. Brugger, *Adv. Mater.* **2012**, *24*, 391-396; d) T. Xu, J. Jin, C. Gregory, J. J. Hickman, T. Boland, *Biomaterials* **2005**, *26*, 93-99; e) X. Cui, T. Boland, *Biomaterials* **2009**, *30*, 6221-6227.

[5] a) R. Censi, W. Schuurman, J. Malda, G. di Dato, P. E. Burgisser, W. J. A. Dhert, C. F. van Nostrum, P. di Martino, T. Vermonden, W. E. Hennink, *Adv. Funct. Mater.* **2011**, *21*, 1833-1842; b) K. Nagahama, T. Ouchi, Y. Ohya, *Adv. Funct. Mater.* **2008**, *18*, 1220-1231; c) M. Chaouat, C. Le Visage, W. E. Baille, B. Escoubet, F. Chaubet, M. A. Mateescu, D. Letourneur, *Adv. Funct. Mater.* **2008**, *18*, 2855-2861; d) J. Malda, J. Visser, F. P. Melchels, T. Jüngst, W. E. Hennink, W. J. A. Dhert, J. Groll, D. W. Hutmacher, *Adv. Mater.* **2013**, *25*, 5011-5028.

[6] a) N. C. Seeman, *Nature* **2003**, *421*, 427-431; b) S. Peng, T. L. Derrien, J. Cui, C. Xu, D. Luo, *Mater. Today* **2012**, *15*, 190-194; c) D. Liu, E. Cheng, Z. Yang, *NPG. Asia Mater.* **2011**, *3*, 109-114; d) Y. Dong, Z. Yang, D. Liu, *Acc. Chem. Res.* **2014**, *47*, 1853-1860; e) S. Modi, M. G. Swetha, D. Goswami, G. D. Gupta, S. Mayor, Y. Krishnan, *Nat. Nanotech.* **2009**, *4*, 325-330; f) A. V. Pinheiro, D. Han, W. M. Shih, H. Yan, *Nat. Nanotech.* **2011**, *6*, 763-772; g) J. Bath, A. J. Turberfield, *Nat. Nanotech.* **2007**, *2*, 275-284; h) Y. Ke, L. L. Ong, W. M. Shih, P. Yin, *Science* **2012**, *338*, 1177-1183; i) N. Chen, J. Li, H. Song, J. Chao, Q. Huang, C. Fan, *Acc. Chem. Res.* **2014**, *47*, 1720-1730.

[7] a) S. H. Um, J. B. Lee, N. Park, S. Y. Kwon, C. C. Umbach, D. Luo, *Nat. Mater.* **2006**, *5*, 797-801; b) B. Wei, I. Cheng, K. Q. Luo, Y. Mi, *Angew. Chem.* **2008**, *120*, 337-339; *Angew. Chem. Int. Ed.* **2008**, *47*, 331-333; c) E. Cheng, Y. Xing, P. Chen, Y. Yang, Y. Sun, D. Zhou, L. Xu, Q. Fan, D. Liu, *Angew. Chem.* **2009**, *121*, 7796-7799; *Angew. Chem. Int. Ed.* **2009**, *48*, 7660-7663; d) Z. Zhu, C. Wu, H. Liu, Y. Zou, X. Zhang, H. Kang, C. J. Yang, W. Tan, *Angew. Chem.* **2010**, *122*, 1070-1074; *Angew. Chem. Int. Ed.* **2010**, *49*, 1052-1056; e) Y. Xing, E. Cheng, Y. Yang, P. Chen, T. Zhang, Y. Sun, Z. Yang, D. Liu, *Adv. Mater.* **2011**, *23*, 1117-1121; f) J. Jin, Y. Xing, Y. Xi, X. Liu, T. Zhou, X. Ma, Z. Yang, S. Wang, D. Liu, *Adv. Mater.* **2013**, *25*, 4714-4717; g) P. Chen, C. Li, D. Liu, Z. Li, *Macromolecules* **2012**, *45*, 9579-9584; h) H. Qi, M. Ghodousi, Y. Du, C. Grun, H. Bae, P. Yin, A. Khademhosseini, *Nat. Commun.* **2013**, *4*; i) C. Li, P. Chen, Y. Shao, X. Zhou, Y. Wu, Z. Yang, Z. Li, T. Weil, D. Liu, *Small* **2014**, DOI: 10.1002/smll.201401906; j) J. Liu, *Soft Matter*, **2011**,*7*, 6757-6767; k) Y. Wu, C. Li, F. Boldt, Y. Wang, S. L. Kuan, T. T. Tran, V. Mikhalevich, C. Fortsch, H. Barth, Z. Yang, D. Liu, T. Weil, *Chem. Commun.* **2014**, DOI: 10.1039/C4CC07144A; l) E. Cheng, Y. Li, Z. Yang, Z. Deng, D. Liu, *Chem. Commun.* **2011**, *47*, 5545-5547.

[8] N. Park, S. H. Um, H. Funabashi, J. Xu, D. Luo, *Nat. Mater.* **2009**, *8*, 432-437.

[9] N. Dave, M. Y. Chan, P.-J. J. Huang, B. D. Smith, J. Liu, *J. Am. Chem. Soc.* **2010**, *132*, 12668-12673.

[10] A. Faulkner-Jones, S. Greenhough, J. A. King, J. Gardner, A. Courtney, W. Shu, *Biofabrication* **2013**, *5*, 015013.

[11] L. Yang, A. R. Dun, K. J. Martin, Z. Qiu, A. Dunn, G. J. Lord, W. Lu, R. R. Duncan, C. Rickman, *PLoS One* **2012**, *7*, e49514.

[12] Y.-C. Chiu, J. C. Larson, V. H. Perez-Luna, E. M. Brey, *Chem. Mater.* **2009**, *21*, 1677-1682.

Entry for the Table of Contents

COMMUNICATION

A rapid-formed supramolecular polypeptide-DNA hydrogel was prepared and applied for *in-situ* multi-layer 3D bioprinting. Based on layer-by-layer alternative deposition stratergy and the self-healing property, the printed structures are geometrically uniform without obvious boundaries. Owing to the high mechanical strength, non-swelling/shrinking properties, the printed structures can keep their shapes without collapse or deformation. Cell printing is demonstrated to produce living-cell-containing structures with high viability and normal cellular functions. Full biodegradability by protease and nuclease provides the possibility of complete removal of hydrogel networks on-demand from systems. All these properties above make the hydrogel a promising bioprinting material for fabrication of desired complex 3D tissue-like constructs with cells for tissue engineering applications.

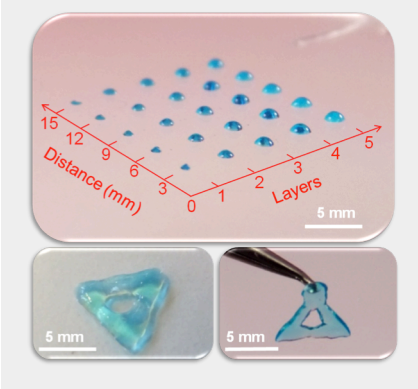

Chuang Li, Alan Faulkner-Jones, Alison R. Dun, Juan Jin, Ping Chen, Yongzheng Xing, Zhongqiang Yang, Zhibo Li, Wenmiao Shu, Dongsheng Liu* and Rory R. Duncan*

Page No. – Page No.

A Rapid-formed Supramolecular Polypeptide-DNA Hydrogel for *in-situ* Multi-layer 3D Bioprinting